JOURNAL OF MATERIALS SCIENCE 28 (1993) 2893–2897

Magnetic and thermal properties of amorphous Al–Gd–TM (TM=Fe, Cu) alloys

R. A. DUNLAP, V. SRINIVAS*, G. BEYDAGHYAN‡
Department of Physics, Dalhousie University, Halifax, Nova Scotia, Canada B3H 3J5
M. E. McHENRY
Department of Metallurgical Engineering and Materials Science, Carnegie-Mellon University, Pittsburgh, PA 15213, USA

Amorphous aluminium–transition metal–rare earth alloys (Al–RE–TM) with compositions $Al_{65}Gd_{15}Cu_{20}$ and $Al_1Gd_1Fe_1$ have been prepared by melt spinning. X-ray diffraction studies show the average interatomic spacing in these alloys to be about 7% greater than in fcc aluminium and about 20% greater than in amorphous Al–TM–Si alloys. Thermal analysis measurements of the $Al_{65}Gd_{15}Cu_{20}$ and $Al_1Gd_1Fe_1$ alloys show the crystallization temperatures to be 647 and 945 K, respectively. Magnetization studies show $Al_{65}Gd_{15}Cu_{20}$ to be paramagnetic with a localized gadolinium moment of $8.0 \pm 0.2\ \mu_B$. $Al_1Gd_1Fe_1$ shows ferromagnetic behaviour, with $T_c = 275$ K and a saturation magnetization of 124 e.m.u. g^{-1}. A room-temperature ^{57}Fe Mössbauer spectrum of $Al_1Gd_1Fe_1$ shows a well-defined quadrupole doublet with a mean splitting of about 0.4 mm s^{-1}. At 77 K, the Mössbauer spectrum shows a well-resolved sextet, corresponding to a mean iron hyperfine field of 96 kOe.

1. Introduction

Transition metal-based amorphous alloys have been studied extensively during the past decade or so. Much of this work has been motivated by possible commercial applications which utilize their unusual mechanical properties, their superior soft magnetic properties, and their ability to absorb large quantities of hydrogen. Amorphous aluminium-based alloys have been known since the early 1980s in Al–TM–M (TM = transition metal, and M = metalloid) alloys [1, 2]. As these alloys are typically very brittle and are only weakly paramagnetic, there was little interest in the possibility of developing commercially viable aluminium-based amorphous alloys. In recent years, however, the situation has changed with the discovery of amorphous Al–RE–TM (RE = rare-earth) alloys which exhibit exceptional tensile strength [3–7]. The principal difficulty in utilizing these materials comes from their low thermal stability. More recently, a class of amorphous Al–RE–TM alloys, which exhibits strong magnetic properties, has been discovered [8, 9]. In the present work we studied the physical properties of two new Al–Gd–TM alloys which exhibit unusual magnetic and thermal properties.

2. Experimental procedure

Samples of the composition $Al_{65}Gd_{15}Cu_{20}$ and $Al_1Gd_1Fe_1$ were prepared by arc-melting high-purity elemental constituents followed by rapid quenching on to a single copper roller with a surface velocity of ~ 60 m s^{-1}. All samples were investigated using CuK_α X-ray powder-diffraction methods on a Siemens D500 scanning diffractometer. The thermal properties of all samples were studied using a Fisher 260F thermal analyser with a heating rate of 20 K min^{-1}. Magnetization was measured as a function of temperature using a SHE superconducting quantum interference device (SQUID) magnetometer with an external d.c. field of 1 T. ^{57}Fe Mössbauer effect spectra were obtained at various temperatures using a $Pd^{57}Co$ source, and a conventional constant acceleration spectrometer with an intrinsic iron linewidth of 0.23 mm (full width at half maximum, FWHM).

3. Results

3.1. X-ray diffraction studies

X-ray diffraction results have shown the as-quenched alloys to be amorphous, with no indication of crystalline peaks. This puts an upper limit of about 0.5% on the concentration of any crystalline phases. The location of the first major diffuse peak gives the mean interatomic spacing in the amorphous structure, $\langle d \rangle$, as given in Table I. The anomalously large values of $\langle d \rangle$ result from the presence of rare-earths in these alloys. As anticipated, the Al–Gd–Cu alloy, which contains 65 at % Al shows a somewhat smaller $\langle d \rangle$ than the Al–Gd–Fe alloy, which contains only 33 at % Al.

* *Present address*: Low Temperature Physics Division, Tata Institute for Fundamental Research, Bombay, India 400 005.
‡ *Present address*: Department of Physics, University of British Columbia, Vancouver, BC, Canada V6T 1A6.

0022–2461

TABLE I Location of the first major diffraction peak (CuK_α radiation), 2θ, with the mean interatomic spacing for a dense random packing of atoms structure $\langle d \rangle = \sqrt{6}\lambda/(4\sin\theta)$. Also given are the temperatures at which crystallization occurs, T_x, as described in Section 3.2. Results are given for various amorphous aluminium-based alloys and fcc aluminium

Alloy	2θ (deg)	$\langle d \rangle$ (nm)	T_x(K)	Reference
$Al_{65}Gd_{15}Cu_{20}$	36.39	0.3022	647	Present work
$Al_1Gd_1Fe_1$	35.38	0.3105	945	Present work
$Al_{90}Fe_5Ce_5$	37.95	0.2902	543	[9]
$Al_{50}Mn_{20}Si_{30}$	46.11	0.2409	676	[10]
fcc Al	–	0.2863	–	–

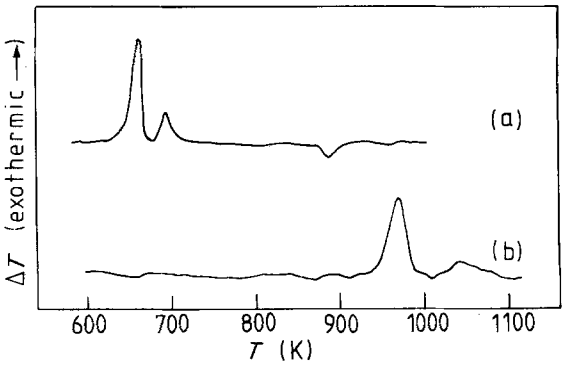

Figure 1 Thermal analysis scans obtained at a heating rate of 20 K min^{-1} for (a) $Al_{65}Gd_{15}Cu_{20}$, and (b) $Al_1Gd_1Fe_1$.

3.2. Thermal analysis studies

Differential thermal analysis (DTA) scans of the alloys studied here are illustrated in Fig. 1. The alloys show crystallization with onsets as given in Table I. Amorphous $Al_{90}Ce_5Fe_5$ and similar alloys, reported previously [3–6], show unusually high tensile strength but anomalously low values of the crystallization temperature. The alloys studied here show much greater thermal stability with crystallization temperatures of up to 945 K (for Al–Gd–Fe). Unfortunately, these alloys, show relatively poor ductility.

3.3. Magnetic susceptibility

The magnetic susceptibility of amorphous Al–Gd–Cu and Al–Gd–Fe as a function of temperature is illustrated in Fig. 2. Results for Al–Gd–Cu show typical Curie paramagnetic behaviour. These data were fit to a susceptibility, $\chi = M/H$, of the form

$$\chi = C/(T - \theta) \quad (1)$$

where the Curie constant is given as

$$C = n\mu_{eff}^2/3k_B \quad (2)$$

where n is the concentration of magnetic ions (gadolinium) per unit volume, μ_{eff} is the effective paramagnetic moment per ion, and k_B is the Boltzmann constant. A fit to the data yields parameters $\theta = 12 \pm 1$ K and $\mu_{eff} = 8.0 \pm 0.2\ \mu_B$. The value of μ_{eff} is consistent with the expected 4f contribution due to the gadolinium ions.

The magnetization of $Al_1Gd_1Fe_1$, as shown in Fig. 2c, shows the existence of strong ferromagnetism with a Curie temperature $T_c = 275$ K. The saturation magnetization in an applied field of 1 T is 124 e.m.u. g^{-1}. This is substantially greater than the largest values of saturation magnetization observed in aluminium-based quasicrystals where the moment is associated with manganese [11, 12]. These ferromagnetic quasicrystals, as well as other amorphous aluminium-based ferromagnets [13], show a deviation of the field-cooled and zero-field-cooled magnetization at low temperature, characteristic of re-entrant spin-glass behaviour [13, 14]. Associated with this is the existence of non-Brillouin magnetization behaviour, particularly at low temperatures. The present $Al_1Gd_1Fe_1$ amorphous alloy shows a conventional ferromagnetic

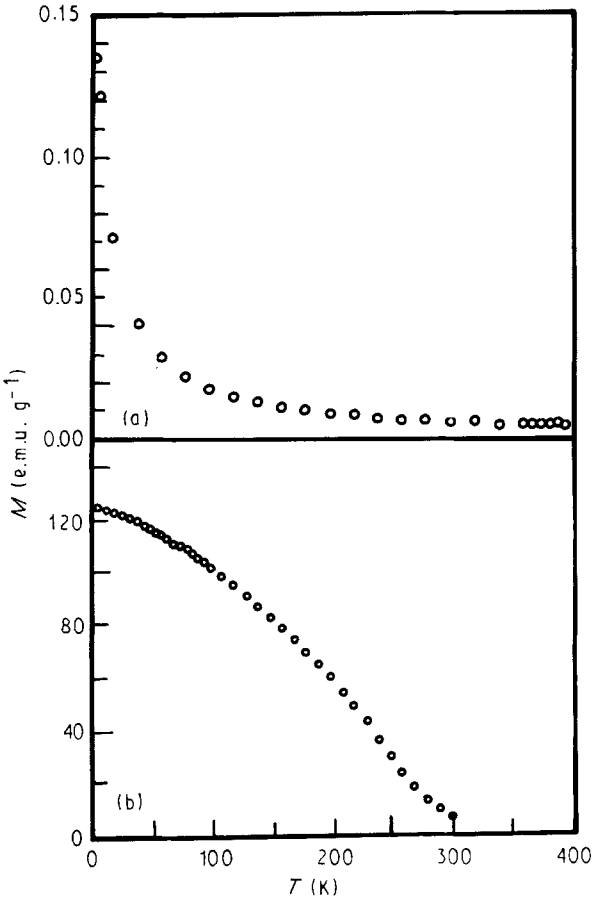

Figure 2 Magnetization as a function of temperature for (a) $Al_{65}Gd_{15}Cu_{20}$, and (b) $Al_1Gd_1Fe_1$ measured in an externally applied field of 1 T.

magnetization curve and no distinction between field-cooled and zero-field-cooled magnetizations, even in an applied field of 1 T at low temperature. The existence of two potentially moment-carrying species in this alloy, iron and gadolinium, does not allow us to extract specific moment values from the magnetization measurements.

3.4. Room-temperature Mössbauer effect studies

A room-temperature ^{57}Fe Mössbauer effect spectrum for Al–Gd–Fe is illustrated in Fig. 3. As we would

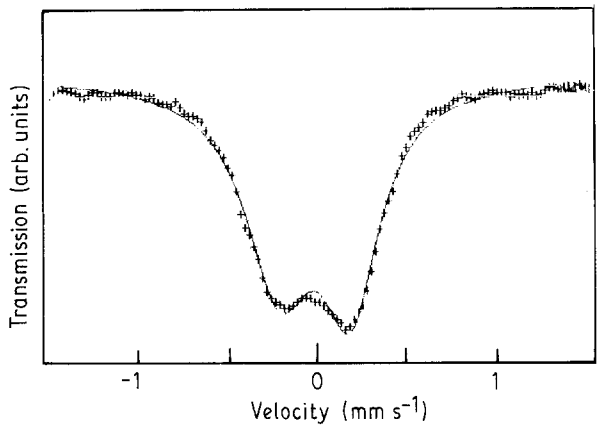

Figure 3 Room-temperature ^{57}Fe Mössbauer effect spectra of $Al_1Gd_1Fe_1$. The solid curve is a fit using the LeCaer–Dubois method.

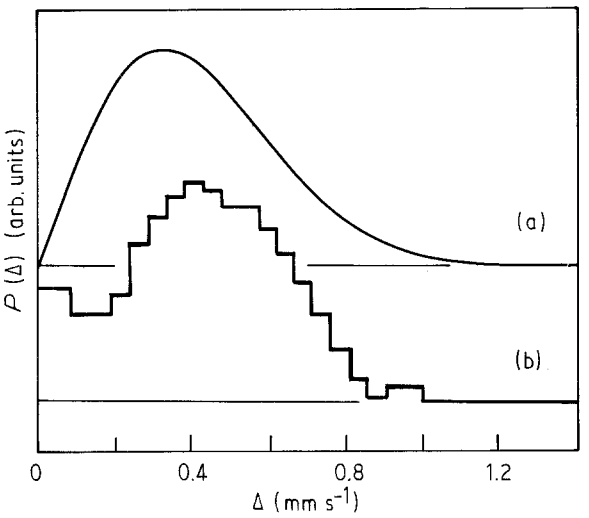

Figure 4 Quadrupole splitting distribution obtained at room temperature for amorphous $Al_1Gd_1Fe_1$ using (a) the shell model, and (b) the model of LeCaer and Dubois.

expect on the basis of the magnetization studies, this alloy shows a quadrupole split doublet at room temperature. The suitability of two different methods of analysis for the present spectrum has been considered. Firstly, we have used the shell method proposed by Czjzek [15]. This expands the distribution of quadrupole splittings, $P(\Delta)$, as

$$P(\Delta) \propto (\Delta/\sigma)^n \exp(-\Delta^2/2\sigma^2) \quad (3)$$

where σ and n are fitted parameters. The parameter n was introduced by Eibschutz *et al.* [16] to account for the short-range order present in disordered materials, e.g. quasicrystals. In the present case, spectral asymmetry is taken into account by a correlation between the isomer shift, δ, and the quadrupole splitting of the form

$$\delta(\Delta) = \delta_0 + \alpha\Delta \quad (4)$$

where δ_0 and α are fitted parameters. For the shell model, the mean quadrupole splitting is given in terms of the fitted parameters as [17]

$$\bar{\Delta} = \sqrt{2}\sigma\Gamma((n+2)/2)/\Gamma((n+1)/2) \quad (5)$$

where $\Gamma(x)$ is the Riemann gamma function.

Secondly, we have used the method of LeCaer and Dubois [18] to fit the distribution of quadrupole interactions. This method makes no a priori assumption about the functional form of $P(\Delta)$, but rather expands this distribution as a set of discrete points. In this case, as well, isomer shift–quadrupole splitting correlations were accounted for by Equation 4.

Parameters obtained from these fits are given in Table II and the resulting quadrupole splitting distributions are illustrated in Fig. 4. While both methods yield consistent values for the parameters, the quadrupole splitting distributions show distinct differences in the shape of the distribution near zero splitting. The LeCaer–Dubois method, which places no constraints on the shape of the distribution, shows a $P(\Delta)$ which is non-zero for $\Delta \to 0$. The functional form of the shell distribution requires that $P(\Delta) \to 0$ as $\Delta \to 0$. Thus the shape of this distribution, at least in the small splitting region, is not consistent with that obtained by the more objective LeCaer–Dubois method. This feature has been observed in the ^{57}Fe quadrupole splitting distributions of a number of other disordered aluminium-based alloys [17]. It is interesting to note, as well, that the value of n from the shell model is near unity. Dunlap *et al.* [19] have suggested that this is characteristic of the lack of structural order found in amorphous materials.

TABLE II Parameters obtained from different fitting methods for room-temperature ^{57}Fe Mössbauer effect spectra of amorphous Al–Gd–Fe. All velocities are in mm s^{-1} and are $\pm$ 0.005 mm s^{-1}. Isomer shifts are measured relative to room temperature α-Fe. Fitting parameters are described in the text.

Parameter	Shell	LeCaer–Dubois
σ	0.325	–
n	1.05	–
$\bar{\Delta}$	0.413	0.409
α	−0.09	−0.09
δ_0	+0.031	+0.029

3.5. Low-temperature Mössbauer effect studies

The liquid nitrogen temperature spectrum of amorphous $Al_1Gd_1Fe_1$, as illustrated in Fig. 5, shows clear magnetic splitting. As is appropriate for the spectra of disordered ferromagnets, we have fit this spectrum to a distribution of hyperfine fields. In this case, we have expanded the distribution, $P(H)$, as a Fourier series using the method of Window [20, 21]. This analysis yields the $P(H)$ shown in Fig. 5 and a mean hyperfine splitting of 96 kOe with an FWHM of the distribution of 92 kOe.

4. Discussion

We have shown that aluminium-based alloys containing as much as 33 at % rare-earth and 33 at % transition metal can be prepared as single-phase amorphous materials by melt spinning. The resulting

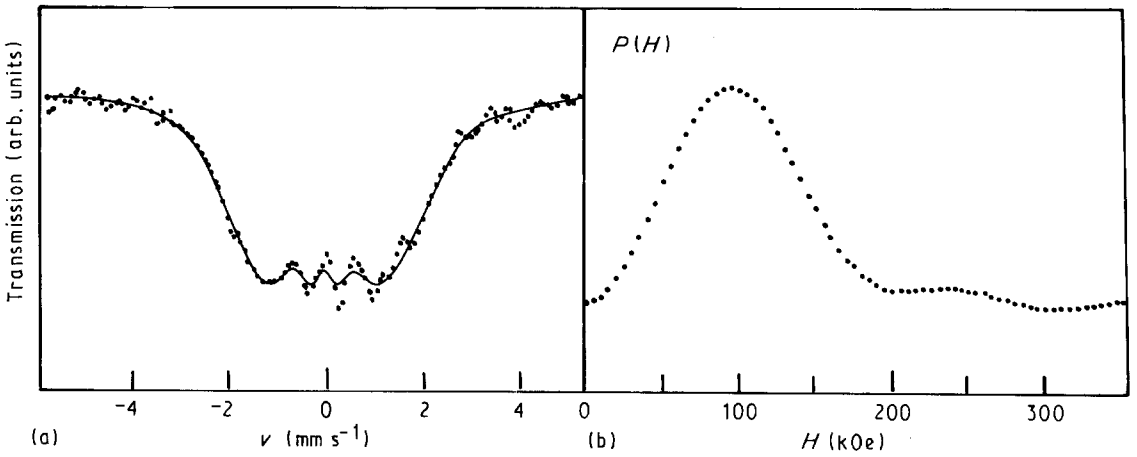

Figure 5 (a) ^{57}Fe Mössbauer effect spectrum of $Al_1Gd_1Fe_1$ obtained at 77 K, and (b) the hyperfine field distribution, $P(H)$, obtained from the spectrum using the method of Window [20], using eight Fourier coefficients and relative line intensities of 3.0:1.1:1.0:1.0:1.1:3.0.

alloys are brittle but show much greater thermal stability than previously studied amorphous Al–TM–Si and high aluminium-content Al–RE–TM alloys. This substantial increase in crystallization temperature suggests the possibility of preparing amorphous Al–RE–TM alloys with sufficient thermal stability to allow for commercial utilization.

The paramagnetic properties of Al–Gd–Cu results from the presence of a large ($\sim 8\ \mu_B$) gadolinium moment. In the case of Al–Gd–Fe, it is difficult, on the basis of the present measurements, to establish the size and location of the magnetic moments. Previous studies of amorphous $Al_{43}Gd_{57}$ [22] have shown a gadolinium moment of 6.5 μ_B and a Curie temperature of ~ 90 K. The present alloys show a smaller gadolinium content and a higher T_c; this suggests the existence of an iron moment with a net positive Gd–Fe coupling. In contrast to the results for ferromagnetic Al–Mn–based quasicrystals and amorphous alloys, the present alloy shows no indication of re-entrant spin glass behaviour and this feature presumably indicates the existence of long-range colinear ferromagnetic order. The present Mössbauer effect results also show the first occurrence of a large iron hyperfine field in this type of material. The presence of such a field indicates: (1) the existence of a substantial localized iron moment, (2) the existence of a strong ferromagnetic coupling between these moments, and (3) a spin arrangement characteristic of a well-ordered ferromagnetic state. The conventional relationship between the iron hyperfine field and the localized magnetic moment, $\sim 140\ \text{kOe}/\mu_B$, suggests an iron moment in this alloy of $\sim 0.7\ \mu_B$ at 77 K.

The width of the iron hyperfine field distribution is indicative of the distribution of iron environments in the alloy. The field distribution in Al–Gd–Fe is consistent with that seen in typical iron-based metallic glasses (e.g. [23]) and suggests that the general features of the short-range order in these two classes of alloys are similar. This is also consistent with the value of n obtained from the fit to the spectrum above T_c to the shell model.

These observations are consistent with the picture of Al–Gd–Fe as a conventional amorphous ferromagnet with long-range colinear spin ordering.

The relationship of the alloys studied here to ferromagnetic quasicrystalline alloys of similar composition and stoichiometry (e.g. [8]) can provide important information on the effects of atomic structure on ferromagnetic order. A substantially larger interatomic spacing, as well as the existence of large moments associated with rare-earth ions are, no doubt, contributing factors, but their specific roles are not clear. Certainly, the existence of a number of Al–RE–TM amorphous and quasicrystalline alloy systems [8, 9], some of which can be prepared over a wide range of compositions, provides a convenient means for the further study of these properties.

Acknowledgement

This work was supported by grants from the Natural Sciences and Engineering Research Council of Canada.

References

1. A. INOUE, A. KITAMURA and T. MASUMOTO, *J. Mater. Sci.* **16** (1989) (1981).
2. R. O. SUZUKI, Y. KOMATSU, K. E. KOBAYASKI and P. H. SINGU, *ibid.* **18** (1985) 1195.
3. A. INOUE, K. OHTERA, A. P. TSAI and T. MASUMOTO, *Jpn J. Appl. Phys.* **27** (1988) L479.
4. A. INOUE, K. OHTERA, A. P. TSAI, H. KIMURA and T. MASUMOTO, *ibid.* **27** (1988) L1579.
5. A. INOUE, K. OHTERA, K. KITA and T. MASUMOTO, *ibid.* **27** (1988) L1796.
6. Y. HE, S. J. POON and G. J. SHIFTET, *Science* **241** (1988) 1640.
7. R. A. DUNLAP, M. YEWONDWOSSEN, V. SRINIVAS, I. A. CHRISTIE, M. E. McHENRY and D. J. LLOYD, *J. Phys. Condens. Matter* **2** (1990) 4315.
8. J. G. ZHOU, private communication (1989).
9. V. SRINIVAS and R. A. DUNLAP, unpublished (1989).
10. R. A. DUNLAP, M. E. McHENRY, V. SRINIVAS, D. BAHADUR and R. C. O'HANDLEY, *Phys. Rev. B* **39** (1989) 4808.
11. M. E. McHENRY, R. A. DUNLAP, V. SRINIVAS and H. LESSURE, unpublished (1990).
12. R. A. DUNLAP, V. SRINIVAS and M. E. McHENRY, *Phys. Rev. B* (1990) submitted.
13. H. FUKAMICHI, T. GOTO, H. WAKABAYASHI, Y. BIZEN, A. INOUE and T. MASUMOTO, *Sci. Reports RITU A* **34** (1988) 93.

14. R. CHATTERJEE, R. A. DUNLAP, V. SRINIVAS and R. C. O'HANDLEY, *Phys. Rev. B* **42** (1990) 2337.
15. G. CZJĘZEK, *ibid.* **25** (1982) 4908.
16. M. EIBSCHUTZ, H. S. CHEN and J. J. HAUSER, *Phys. Rev. Lett.* **56** (1986) 169.
17. D. W. LAWTHER, R. A. DUNLAP, V. SRINIVAS, D. J. LLOYD and S. JHA, *Hyperf. Interact.* **60** (1990) 785.
18. G. LeCAER and M. DUBOIS, *J. Phys. E Sci. Instrum.* **12** (1979) 1083.
19. R. A. DUNLAP, R. C. O'HANDLEY, M. E. McHENRY and V. SRINIVAS, *Struct. Chem.* **2** (1991) 501.
20. B. WINDOW, *J. Phys. E Sci. Instrum.* **4** (1971) 401.
21. R. A. DUNLAP and S. P. RITCEY, *Phys. Rev. B* **32** (1985) 3325.
22. V. SKUMRYEV, H. GAMARI-SEALE, D. X. CHEN, K. V. RAO and A. APOSTOLOV, *J. de Phys.* **49** (1988) C8-1363.
23. R. A. DUNLAP, *J. Phys. F Met. Phys.* **14** (1984) 549.

Received 9 September 1991
and accepted 24 July 1992